

# Thermodynamic Measurements on $\text{CH}_3\text{CCl}_3$ , $(\text{CH}_3)_2\text{CBr}_2$ , and on $n\text{C}_{20}\text{H}_{42}$ at High Pressures

Albert Würflinger and Luis Carlos Pardo<sup>a</sup>

Institute of Physical Chemistry II, Ruhr-University, D-44780 Bochum

<sup>a</sup> Departament de Física i Enginyeria Nuclear (ETSEIB), UPC, Universitat Politècnica de Catalunya, Diagonal 647, 08028 Barcelona, Catalonia (Spain)

Reprint requests to Prof. A. W.; Fax: 0234-32-14183;

E-mail: Albert.Wuerflinger@ruhr-uni-bochum.de

Z. Naturforsch. **57 a**, 177–183 (2002); received February 27, 2002

1,1,1-Trichloroethane ( $\text{CH}_3\text{CCl}_3$ ), 2,2-Dibromopropane ( $(\text{CH}_3)_2\text{CBr}_2$ ), and Eicosane ( $n\text{C}_{20}\text{H}_{42}$ ) have been investigated with differential thermal analysis (DTA) under high pressure using compressed argon and helium as a pressure medium. In the case of the chemically reactive halogenated samples the measurements were performed in open DTA containers. It was found that compressed helium modified the phase boundaries much less than compressed argon. In the case of eicosane there was no reaction with the DTA containers, and the measurements performed in closed containers were well reproducible, independent of the pressurized gas used. Furthermore  $pVT$  measurements have been carried out in the neighbourhood of the melting region for  $\text{CH}_3\text{CCl}_3$  and  $(\text{CH}_3)_2\text{CBr}_2$ . The  $pVT$  measurements yield the volume change of melting, from which the enthalpy change is calculated with the aid of the Clausius-Clapeyron equation. The specific volumes of the solid phases below the melting point are compared with crystallographic data.

**Key words:** Plastic Crystals; Eicosane; DTA;  $pVT$ ; Phase Transition; High Pressure.

## 1. Introduction

DTA and  $pVT$  measurements are suitable experimental methods for the study of the phase behaviour of plastic crystals [1, 2]. In particular tert-butyl compounds, which have an approximate

globular shape [3], have been extensively investigated [4 - 6]. The methylchloromethane compounds,  $(\text{CH}_3)_{4-n}\text{CCl}_n$  ( $n = 2 - 4$ ), belong to this class of materials displaying two orientationally disordered phases (ODIC) with two melting points [7]. Recently one representative, 1,1,1-trichloroethane ( $\text{CH}_3\text{CCl}_3$ ), was used as a component in the determination of binary phase diagrams [8, 9]. In Fig. 1 we present a DSC study for  $\text{CH}_3\text{CCl}_3$  at normal pressure. On cooling the monotropic ODIC phase Ia (fcc) is formed, which transforms into another ODIC phase Ib (rhomboedric) which, on further cooling, yields the ordered phase II (orthorhombic). On reheating crystal II transforms to the disordered phase Ib that remains stable up to the melting point (which is ca. 5 K higher than the melting point of Ia).

No high-pressure measurements have been reported for  $\text{CH}_3\text{CCl}_3$ . However, for another homologue, 2,2-dichloropropane, the pressure phase diagram has been established [10]. The slope of the melting curve for Ia enabled us to determine the volume change and hence the density of the solid state, from which

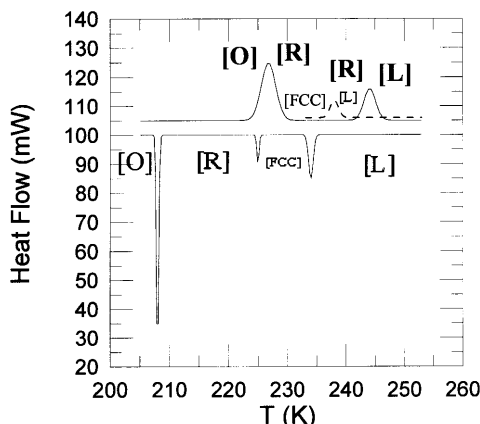


Fig. 1. DSC thermogram of  $\text{CH}_3\text{CCl}_3$  at normal pressure.

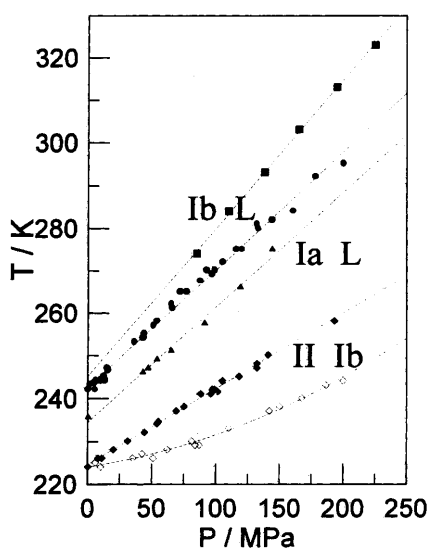


Fig. 2.  $p$ - $T$  phase diagram of  $\text{CH}_3\text{CCl}_3$  established with DTA:  $\diamond$ , II $\rightarrow$ Ib under argon;  $\blacklozenge$ , II $\rightarrow$ Ib;  $\blacktriangle$ , Ia $\rightarrow$ L;  $\bullet$ , Ib $\rightarrow$ L, under helium;  $\blacksquare$ , Ib $\rightarrow$ L, established with  $p$ - $V$ - $T$ .

$Z = 20$  could be concluded for the simple cubic crystal lattice symmetry [11]. It would be interesting to compare these properties with the methylbromomethane series. Preliminary measurements in Barcelone on 2,2-dibromo-propane ( $(\text{CH}_3)_2\text{CBr}_2$ ) seemed to reveal both Ia and Ib ODIC phases. In the present paper we have chosen  $\text{CH}_3\text{CCl}_3$  and  $(\text{CH}_3)_2\text{CBr}_2$  for a thermodynamic study under pressure.

N-alkanes ( $\text{C}_n\text{H}_{2n+2}$ ) of mean chain length display one or more rotator phases [12]. They play an important role for energy storage applications [13] and as model substances for theoretical calculations [14] and simulations [15]. Eicosane ( $\text{C}_{20}\text{H}_{42}$ ) is just below the series  $n \geq 22$  of the even  $n$ -alkanes for which a stable rotator phase is observed. It displays a metastable rotator phase on cooling [16]. In the present study we employ DTA under pressure in the neighbourhood of the melting transition.

## 2. Experimental

DTA measurements were carried out with an equipment described in [17, 18]. The samples to be studied are enclosed in small containers which are moulded from indium. Compressed argon or helium are used as pressure medium. The temperature is measured with thermocouples. Thermograms are recorded both on

heating and cooling. In heating runs the temperature increase is adjusted to 1 or  $2 \text{ K} \cdot \text{min}^{-1}$ .

For the  $p$ - $V$ - $T$  measurements a recently established high-pressure dilatometer is employed which allows repeated measurements with the same filling [19, 20]. In general, volume changes are recorded at increasing and decreasing pressure along an isotherm. The corrected raw data (correction for the hysteresis pressure, volume change of the sample holder etc.) are combined with atmospheric pressure data in order to establish specific volumes in the whole  $p$ ,  $T$  range. The densities at ambient pressure are either taken from literature or measured with a vibrating tube density meter Anton Paar.

1,1,1-Trichloroethane was purchased from Aldrich (99%), 2,2-Dibromopropane from Acros (95%). Eicosane came from Aldrich with a purity of 99.3%.

## 3. Results and Discussion

### 3.1. DTA Measurements under Pressure

#### 1,1,1-Trichloroethane

The phase diagram of this compound was published by Figuière et al., who report a splitting of the solid II-I transition at high pressures [21]. However, no details of the phase boundaries were given, nor a monotropic ODIC phase was noted. The authors mention also a solid III-II transition at lower temperatures.

In our DTA study, first test runs in closed containers under compressed argon revealed the melting and solid II-solid Ib transition. However, the well-known monotropic ODIC phase Ia [7] was not well reproduced. Moreover, there was a large scatter of points, and the DTA containers, after being removed from the high-pressure vessel, were corroded. Obviously the sample  $\text{CH}_3\text{CCl}_3$  underwent a chemical reaction with the indium container that made the walls of the capsule porous and enabled the compressed gas to be dissolved in the substance, thus changing the transition temperatures significantly. Therefore we continued with measurements in open containers using both compressed argon and helium to transmit the pressure. It is well known that the influence of dissolved helium on the phase behaviour is distinctly smaller, though still noticeable [22, 23]. Indeed the runs under helium revealed clearly the monotropic phase under pressure. The phase behaviour is presented in Fig. 2, together with results from  $p$ - $V$ - $T$  measurements (see

Table 1. Phase transitions observed with DTA in  $\text{CH}_3\text{CCl}_3$ .

Transition	<i>a</i>	<i>b</i>
$\text{Ib} \rightarrow \text{L}$	242.61	0.277
$\text{Ia} \rightarrow \text{L}$	234.56	0.269
$\text{II} \rightarrow \text{Ib}$	224.7	0.177

Table 2. Phase transitions observed with DTA in  $(\text{CH}_3)_2\text{CBr}_2$ .

Transition	<i>a</i>	<i>b</i>
$\text{I} \rightarrow \text{L}$	255.0	0.32
$\text{II} \rightarrow \text{I}$	214.7	0.129

below) for which the melting curve lies significantly higher. The DTA measurements under helium reveal still a remarkable depression of the melting under pressure. A similar effect was previously noted for the melting of *n*-alkanes, when open containers were used [22].

Due to the chemical reaction of  $\text{CH}_3\text{CCl}_3$  with the sample container the DTA results in Fig. 2 should only be considered as providing the main trends of the phase behaviour. The solid-solid transition under pressurized argon can certainly be disregarded. The phase lines observed under helium pressure are fitted by polynomials of first order

$$T/\text{K} = a + b \cdot (p/\text{MPa}),$$

see Table 1.

#### 2,2-Dibromopropane

Again we started the measurements with closed containers under compressed argon, but the indium containers were much worse corroded than with the  $\text{CH}_3\text{CCl}_3$  sample. Even under compressed helium there was no clear detection of a monotropic ODIC phase. However, the solid solid transition of  $(\text{CH}_3)_2\text{CBr}_2$  could be well reproduced under pressure, see Figure 3. As for  $\text{CH}_3\text{CCl}_3$ , we fit the measurements under helium by polynomials of first order, see Table 2.

#### Eicosane

The pressure dependence of the melting and freezing was measured up to 220 MPa. Runs were performed both under compressed helium and argon in

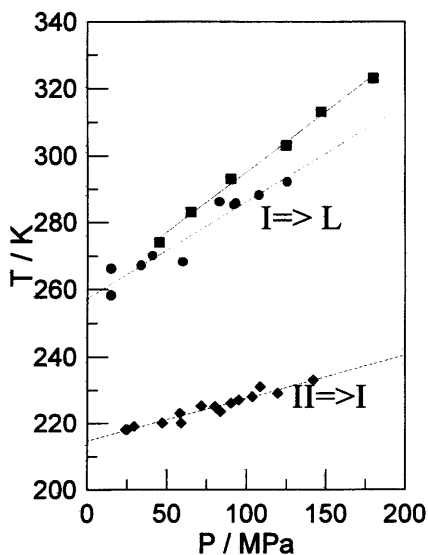


Fig. 3.  $p$ - $T$  phase diagram of  $(\text{CH}_3)_2\text{CBr}_2$  established with DTA:  $\blacklozenge$ ,  $\text{II} \rightarrow \text{I}$ ,  $\bullet$ ,  $\text{I} \rightarrow \text{L}$ , under helium;  $\blacksquare$ ,  $\text{I} \rightarrow \text{L}$ , established with  $pVT$ .

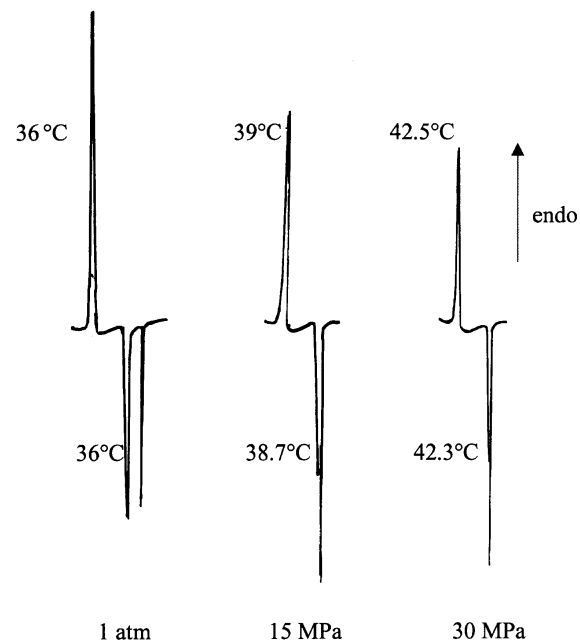


Fig. 4. DTA traces of eicosane, peaks upwards: heating; peaks downwards: cooling showing the monotropic rotator phase.

closed containers, without any differences in the results. Some DTA traces are displayed in Figure 4. On

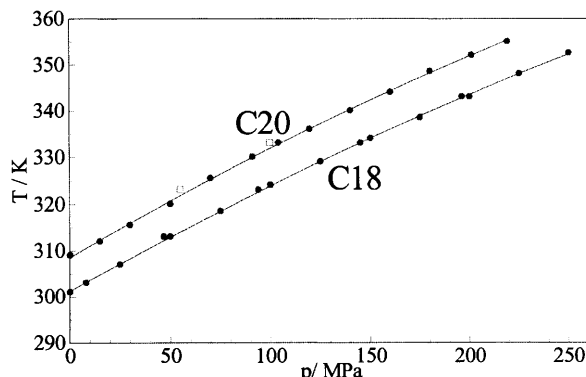


Fig. 5. Melting curve of eicosane compared with octadecane [2], □: freezing points of  $C_{20}H_{42}$  after [25].

heating only the melting is observed, on cooling the main peak (at 1 atm) is preceded by a smaller one, representing the transition to the monotropic rotator phase. At 30 MPa the additional peak appears only as a shoulder. For higher pressures the monotropic transition could not be detected any more. So, the monotropic rotator phase vanishes above a triple point as do the stable rotator phases [22, 24]. The melting curve was fitted to  $T/K = 308.62 + 0.2506 p/\text{MPa} - 1.7 \cdot 10^{-4} (p/\text{MPa})^2$ . In Fig. 5 the melting of  $C_{20}H_{42}$  is compared with that of  $C_{18}H_{38}$  [2], showing that both curves run almost parallel. Another high-pressure study concerns the density of liquid eicosane up to 150 MPa, derived from measurements of the speed of sound [25]. The authors note that at lower temperatures the pressure range was limited to the freezing of eicosane, namely 54.95 MPa at 323.15 K and 99.75 MPa at 333.15 K. These two points (included in Fig. 5) are indeed very close to the DTA melting curve.

Calorimetric data are reported by van Miltenburg et al. [26], according to which the enthalpy of fusion for eicosane amounts to  $69.922 \text{ kJ mol}^{-1}$ . Using the Clausius-Clapeyron equation we calculate a volume change of  $56.6 \text{ cm}^3 \text{ mol}^{-1}$  (or  $0.2 \text{ cm}^3 \text{ g}^{-1}$ ) for the melting. Dutour et al. [25] present the atmospheric pressure densities of  $C_{20}H_{42}$  by a smoothed polynomial, yielding  $v(\text{spec.}) = 1.2858 \text{ cm}^3 \text{ g}^{-1}$  for the liquid at 309.65 K. On the other hand,  $v(\text{spec.})$  may be calculated from crystallographic data (reported for  $T = 291 \text{ K}$  [16]), from which we derive  $V = 506.84 \text{ \AA}^3 \Rightarrow v(\text{spec.}) = 1.0802 \text{ cm}^3 \text{ g}^{-1}$  for the crystal. The difference  $v(\text{liquid}) - v(\text{crystal}) = 0.2056 \text{ cm}^3 \text{ g}^{-1}$  is somewhat larger than the  $\Delta V_{\text{fus}} = 0.2 \text{ cm}^3 \text{ g}^{-1}$  esti-

mated with the aid of the Clausius-Clapeyron equation. But the expansion of the crystal from 291 K to 309.65 K would diminish  $\Delta V_{\text{fus}}$ . Another value for  $\Delta V_{\text{fus}}$  of  $0.2077 \text{ cm}^3 \text{ g}^{-1}$  reported by Templin [27], is still higher.

### 3.2. pVT Measurements

#### 1,1,1-Trichloroethane

For the measurements a dilatometric cell made of stainless steel was used that did not react with the samples. It was checked in previous pVT studies [1, 2, 5, 6] that the same pressure dependence of phase transitions is observed as in DTA measurements with closed containers, provided the samples do not react with the cell material. The specific volumes of  $CH_3CCl_3$  are presented in the Figs. 6a, b for decreasing (melting) and increasing (freezing) pressures, respectively. The steps in Fig. 6 (indicating the volume changes and the transition pressure) are sharper on freezing. However, the monotropic Ia phase was not detected, since freezing occurred almost at the same pressure as melting of phase Ib. For each isotherm (separately for the liquid and the ODIC phase) the  $v(p)$ -curves were fitted to polynomials and then extrapolated to the corresponding transition pressure. Thus we obtain the specific volumes along the melting curve that is displayed in Figure 7. The distance between the two curves is the volume change of melting from which we calculate the enthalpy change with the aid of the Clausius-Clapeyron equation. The melting curve, derived from the pVT measurements, is presented by  $T/K = 242.09 + 0.3933 p/\text{MPa} - 1.469 \cdot 10^{-4} (p/\text{MPa})^2$  and included in Figure 2. The specific volumes along the melting curve are fitted to polynomials of first order:  $v_{\text{liq}}/\text{cm}^3 \text{ g}^{-1} = 0.7010 - 1.394 \cdot 10^{-4} (p/\text{MPa})$ ;  $v_{\text{cr}}/\text{cm}^3 \text{ g}^{-1} = 0.67416 - 9.707 \cdot 10^{-5} (p/\text{MPa})$ ; hence  $\Delta V_{\text{Cr} \rightarrow \text{L}} = 0.02684 \text{ cm}^3 \text{ g}^{-1}$  or  $3.580 \text{ cm}^3 \text{ mol}^{-1}$  at ambient pressure. Using the Clausius-Clapeyron equation and the slope of the melting curve ( $0.3933 \text{ K/MPa}$ ) we calculate  $\Delta H_{\text{Cr} \rightarrow \text{L}} = 2.20 \text{ kJ mol}^{-1}$  in fair agreement with a DSC measurement:  $\Delta H_{\text{Cr} \rightarrow \text{L}} = 2.31 \text{ kJ mol}^{-1}$  [8]. Calculation of the enthalpy changes for higher pressures yielded practically no pressure dependence:  $\Delta H_{\text{Cr} \rightarrow \text{L}} \approx 2.3 (\pm 0.1) \text{ kJ mol}^{-1}$  where both decreasing and increasing pressure runs have been considered. This means that the decrease of the volume change with

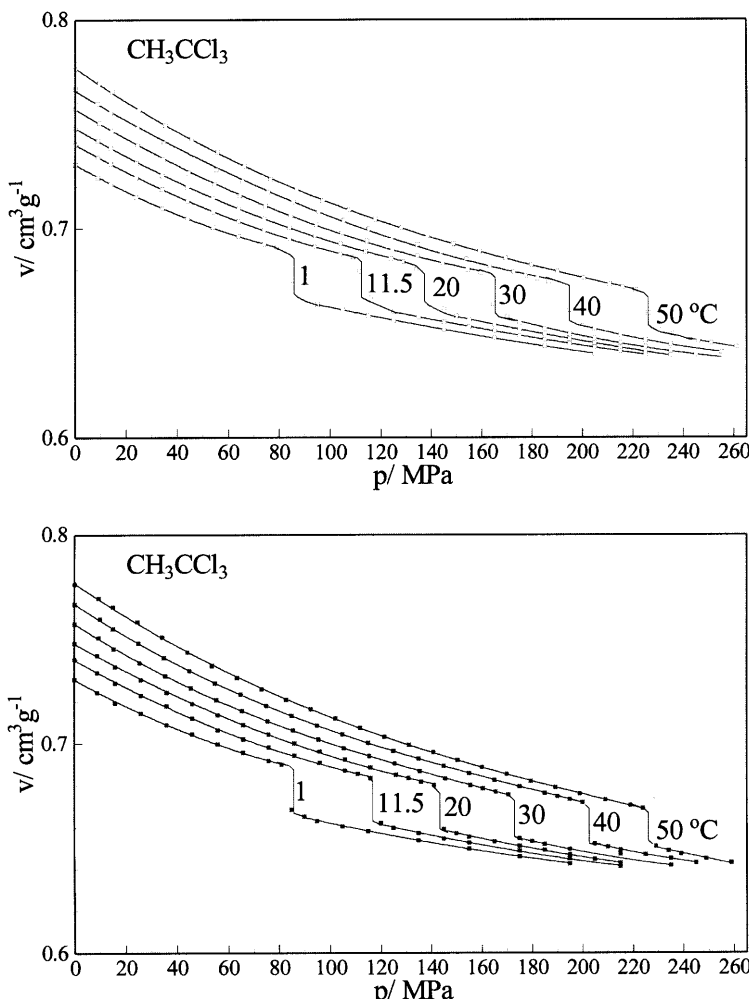


Fig. 6. Specific volumes of  $\text{CH}_3\text{CCl}_3$  as a function of pressure. *top*:  $v(p)$  isotherms at 6 different temperatures (decreasing pressure), *bottom*:  $v(p)$  isotherms at 6 different temperatures (increasing pressure).

rising pressure ( $\Delta V_{\text{Cr} \rightarrow \text{L}} / \text{cm}^3 \text{g}^{-1} = 0.02684 - 4.229 \cdot 10^{-5} (p/\text{MPa})$ ) is compensated by the change of ( $T \cdot dp/dT$ ) of the melting curve.

The specific volumes, extrapolated to atmospheric pressure, may be compared with literature data. For the liquid state, densities are reported by Daubert et al. [28]. The authors mention the equation

$$\rho = 0.129514 / 0.2728^{1+(1-T/545)^{0.2925}}$$

for the liquid density of  $\text{CH}_3\text{CCl}_3$  ( $\rho$  in  $\text{g} \cdot \text{cm}^{-3}$ ,  $T$  in K). The equation was tested with selected values from Beilstein [29], which were also used to link the high-pressure data to 1 atm. At the ambient melting point ( $-31^\circ\text{C}$ ) the density is  $\rho = 1.4176 \text{ g} \cdot \text{cm}^{-3}$ ,  $\Rightarrow v(\text{liq.}) = 0.7054 \text{ cm}^3 \text{g}^{-1}$ . Crystallographic data yield  $v(\text{cr.}) =$

$0.6667 \text{ cm}^3 \text{g}^{-1}$ , that is slightly smaller than  $v(\text{cr.}) = 0.6742 \text{ cm}^3 \text{g}^{-1}$  derived from  $pVT$  measurements.

#### 2,2-Dibromopropane

The specific volumes of  $(\text{CH}_3)_2\text{CBr}_2$  are presented in the Figs. 8a, b for decreasing and increasing pressures, similarly to Figure 6. For this compound no density data were available. Therefore they were determined with a density meter from Anton Paar and fitted to a linear equation (for  $0 < T < 50^\circ\text{C}$ ):  $\rho/\text{g} \cdot \text{cm}^{-3} = 1.8848 - 1.9825 \cdot 10^{-3} T/\text{K}$ . Contrary to  $\text{CH}_3\text{CCl}_3$ , the melting step is much less pronounced due to the large impurity of  $(\text{CH}_3)_2\text{CBr}_2$ . This renders the estimation of  $\Delta V_{\text{Cr} \rightarrow \text{L}}$  particularly difficult. Evaluation of the thermodynamic data as above yielded for the melting curve:  $T/\text{K} = 253.73 + 0.4843 (p/\text{MPa})$

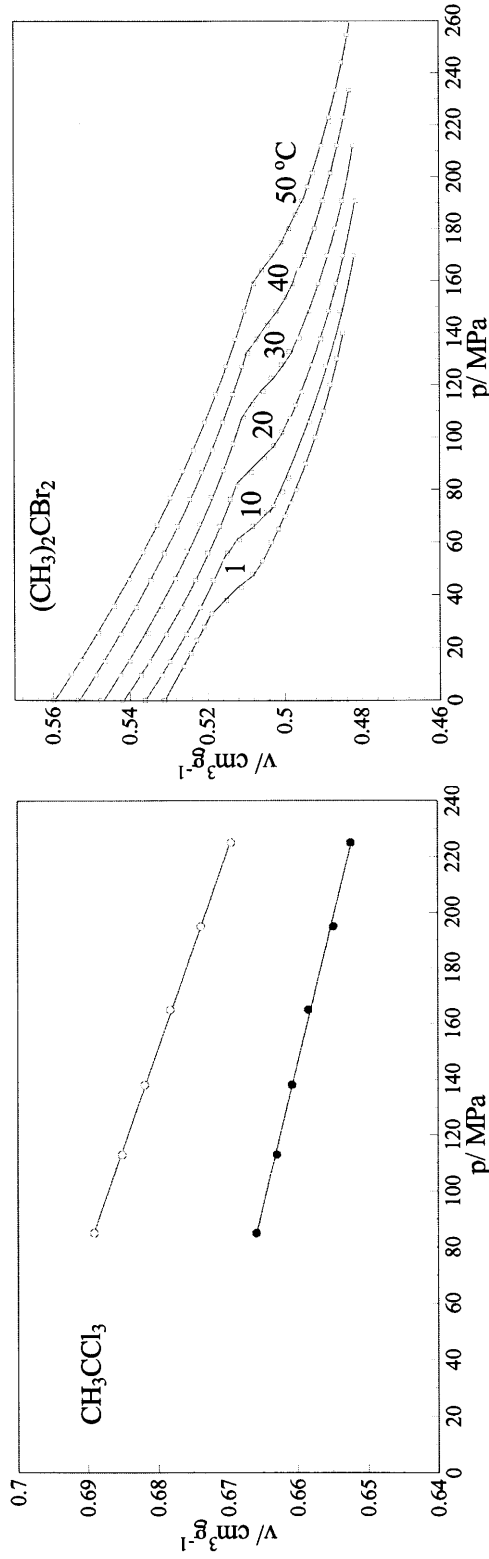


Fig. 7. Specific volumes of  $\text{CH}_3\text{CCl}_3$  along the melting curve,  $\circ$  liquid;  
 ● crystal.

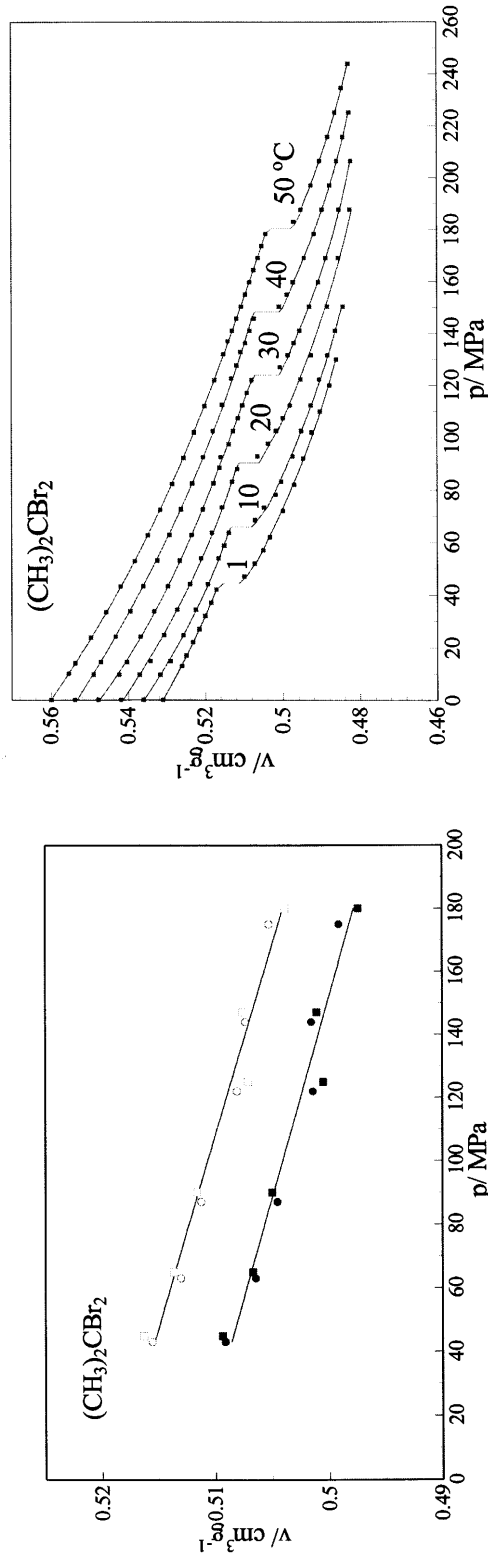


Fig. 8. Specific volumes of  $(\text{CH}_3)_2\text{CBr}_2$  as a function of pressure.  
 top:  $v(p)$  isotherms at 6 different temperatures (decreasing pressure),  
 bottom:  $v(p)$  isotherms at 6 different temperatures (increasing pressure).

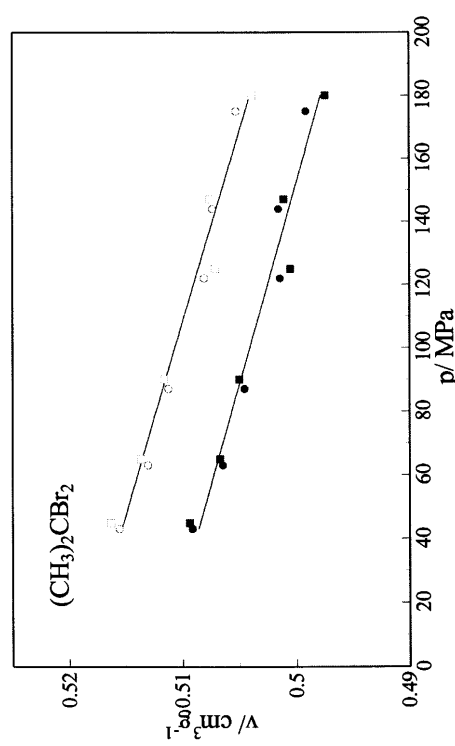


Fig. 9. Specific volumes of  $(\text{CH}_3)_2\text{CBr}_2$  along the melting curve, de-  
 creasing pressure:  $\circ$  liquid, ● crystal; increasing pressure: □ liquid, ■  
 crystal.

–  $5.41 \cdot 10^{-4}$  (p/MPa)<sup>2</sup>; which is compared with the DTA results in Figure 3. The specific volumes along the melting curve are presented by  $v_{\text{liq}}/\text{cm}^3\text{g}^{-1} = 0.5189 - 8.225 \cdot 10^{-5}$  (p/MPa);  $v_{\text{cr}}/\text{cm}^3\text{g}^{-1} = 0.5120 - 7.853 \cdot 10^{-5}$  (p/MPa) and plotted in Fig. 9, which shows a considerable scatter. The volume change on melting ( $\Delta V_{\text{Cr} \rightarrow \text{L}}/\text{cm}^3\text{g}^{-1} = 0.00692 - 3.717 \cdot 10^{-6}$  (p/MPa)) is distinctly smaller than in the case of  $\text{CH}_3\text{CCl}_3$ . However, for  $(\text{CH}_3)_2\text{CBr}_2$   $\Delta V_{\text{Cr} \rightarrow \text{L}}$  is practically independent of pressure, hence  $\Delta H_{\text{Cr} \rightarrow \text{L}}$  (calculated with Clausius-Clapeyron) increases with pressure from 0.8 kJ·mol<sup>-1</sup> at 40 MPa to 1.4 kJ·mol<sup>-1</sup> at 180 MPa. Consequently,  $\Delta H_{\text{Cr} \rightarrow \text{L}} = 0.73$  kJ·mol<sup>-1</sup> at ambient pressure is smallest and disagrees with

$\Delta H_{\text{Cr} \rightarrow \text{L}} = 1.44$  kJ·mol<sup>-1</sup> determined by DSC. Apparently the discrepancies are to a large extent caused by the sluggish melting transition, so that the melting step is not well defined.

#### Acknowledgement

The collaboration was supported by “la Xarxa Temàtica Aliatges Moleculars de la Generalitat de Catalunya” and the “REALM” (Réseau Européen sur les Alliages Moléculaires). One of us (LCP) thanks the state of Catalonia for financial grant 2000BEAI200219. We thank Dr. Denise Mondieig for providing us with a sample of eicosane.

- [1] M. Jenau, M. Sandmann, A. Würflinger, and J. Ll. Tamarit, *Z. Naturforsch.* **52a**, 493 (1997).
- [2] A. Würflinger, D. Mondieig, F. Rajabalee, and M. A. Cuevas-Diarte, *Z. Naturforsch.* **56a**, 626 (2001); Err. *ibid.* p. 895.
- [3] J. Timmermans, *Bull. Soc. Chim. Belges* **44**, 17 (1935); *J. Chim. Physique* **35**, 331 (1938); *J. Phys. Chem. Solids* **18**, 1 (1961).
- [4] N. G. Parsonage and L. A. K. Staveley: *Disorder in Crystals*, Clarendon Press, Oxford 1978; L. A. K. Staveley, *Ann. Rev. Phys. Chem.* **13**, 351 (1962).
- [5] J. Wilmers, M. Briese, and A. Würflinger, *Mol. Cryst. Liq. Cryst.* **187**, 293 (1984).
- [6] J. Reuter, D. Büsing, J. Ll. Tamarit, and A. Würflinger, *J. Mater. Chem.* **7**, 41 (1997).
- [7] L. Silver and R. Rudman, *J. Phys. Chem.* **74**, 3134 (1970); R. Rudman and B. Post, *Mol. Cryst.* **5**, 95 (1968).
- [8] L. C. Pardo, M. Barrio, J. Ll. Tamarit, P. Negrier, D. O. López, J. Salud, and D. Mondieig, *J. Phys. Chem. B* **105**, 10326 (2001).
- [9] L. C. Pardo, M. Barrio, J. Ll. Tamarit, D. O. López, J. Salud, P. Negrier, and D. Mondieig, *Chem. Chem. Phys. Lett.* **308**, 204 (1999).
- [10] P. Negrier, L. C. Pardo, J. Salud, J. Ll. Tamarit, M. Barrio, D. O. López, A. Würflinger, and D. Mondieig, *J. Mater. Chem.*, in press.
- [11] P. Negrier, L. C. Pardo, J. Salud, J. Ll. Tamarit, M. Barrio, D. O. López, A. Würflinger, and D. Mondieig: New insights into the polymorphism of  $(\text{CH}_3)_2\text{CCl}_2$ ; XXVII JEEP, Montpellier, France (2001), Poster, p. 245.
- [12] D. Mondieig, P. Espeau, L. Roblès, Y. Haget, H. A. J. Oonk, and M. A. Cuevas-Diarte, *J. Chem. Soc. Faraday Trans.* **93**, 3343 (1997).
- [13] D. Mondieig, A. Marbeuf, L. Roblès, P. Espeau, P. Poirier, Y. Haget, T. Calvet-Pallas, and M. A. Cuevas-Diarte, *High Temperatures - High Pressures* **29**, 385 (1997).
- [14] A. Würger, *J. Chem. Phys.* **112**, 3897 (2000); *Phys. Rev. Lett.* **83**, 4816 (1999).
- [15] J. P. Ryckaert, M. L. Klein, and I. R. McDonald, *Mol. Phys.* **83**, 439 (1994); Y. Tsuchiya, H. Hasegawa, and T. Iwatsubo, *J. Chem. Phys.* **114**, 2484 (2001).
- [16] P. Espeau, L. Roblès, D. Mondieig, Y. Haget, M. A. Cuevas-Diarte, and H. A. J. Oonk, *J. Chim. Phys.* **93**, 1217 (1996).
- [17] A. Würflinger, *Ber. Bunsenges. Phys. Chem.* **79**, 1195 (1975); N. Pingel, U. Poser, and A. Würflinger, *J. Chem. Soc. Faraday Trans. I*, **80**, 3221 (1984).
- [18] C. Schmidt, M. Rittmeier-Kettner, H. Becker, J. Ellert, R. Krombach, and G. M. Schneider, *Thermochim. Acta* **238**, 321 (1994).
- [19] M. Sandmann, doctoral thesis, Ruhr-University of Bochum, Germany, 1998.
- [20] A. Würflinger, M. Sandmann, and W. Weissflog, *Z. Naturforsch.* **55a**, 823 (2000).
- [21] P. Figuière, R. Guillaume, and H. Szwarc, *J. Chim. Physique* **68**, 124 (1971).
- [22] A. Würflinger and G. M. Schneider, *Ber. Bunsenges. Phys. Chem.* **77**, 121 (1973).
- [23] R. Krombach and G. M. Schneider, *Thermochimica Acta* **231**, 169 (1994).
- [24] P. W. Richter and C. W. F. T. Pistorius, *Mol. Cryst. Liq. Cryst.* **16**, 153 (1972).
- [25] S. Dutour, J. L. Daridson, and B. Lagourette, *High Temp. High Press.* **33**, 371 (2001).
- [26] J. C. Van Miltenburg, H. A. J. Oonk, and V. Métivaud, *J. Chem. Eng. Data* **44**, 715 (1999).
- [27] P. R. Templin, *Ind. Eng. Chem.* **48**, 154 (1956).
- [28] T. E. Daubert and R. P. Danner, “Physical and Thermodynamic Properties of Pure Chemicals”, Data compilation, Taylor & Francis, Washington 1994.
- [29] German data base: CrossFire Beilstein.